9th IAA Planetary Defense Conference – PDC 2025
5-9 May 2025, Stellenbosch, Cape Town, South Africa

IAA-PDC-25-06-229

Options and Uncertainties for Nuclear Mitigation in the 2025 Hypothetical Asteroid Threat Exercise Scenario

Catherine S. Plesko[(1)], Stephen A. Becker[(2)], Mark B. Boslough[(2)], Wendy K. Caldwell[(2)] , and Megan L. Harwell[(2)]
[(1)]*Los Alamos National Laboratory, Mail Stop T082, PO Box 1663, Los Alamos, NM, 87544, USA, plesko@lanl.gov*
[(2)] *Los Alamos National Laboratory, Los Alamos, NM, USA*

Abstract

We propose that a single 1 MT burst near its surface could strongly disrupt the 2024 PDC hypothetical threat object. For perspective, 2024 PDC would be of comparable size and mass to the PDC 2011 conference venue, although the asteroid would be expected to be substantially weaker than a reinforced concrete building. We show from scaling relations calibrated to nuclear tests on Earth and hydrocode models of the scenario that it is plausible that such an object could be disrupted and dispersed by a single device or small number of devices on a rendezvous mission.

Keywords: Deflection, Disruption, Hydrocode, Mitigation, Mission Planning

Introduction

Nuclear devices have often suggested as a tool for preventing PHOs from striking the Earth. There are a variety of ways they could be used, ranging from strong disruption and vaporization of the object [1] to ablating a small portion of the surface regolith without vaporizing it [2]. Strong disruption of the type advocated by Teller et al. [1] fell out of favor because the careful placement of device or extremely high yield requirements drove mission design to extremely challenging or impossible portions of design space such as high-delta-V rendezvous missions by massive spacecraft which were not launchable by vehicles available at the time of those studies. High-speed intercept missions have lower delta-V requirements relative to rendezvous missions but offer limited precision on the height of burst for nuclear mitigation missions and increase the risk of premature impact for missions attempting small heights of burst. Other studies, such as [3], intentionally err on the side of caution by applying a heuristic based on the escape velocity of the target object. They are likely correct that if the impulse from stand-off burst ablation is delta $v < 0.1\ v_{esc}$, the object is very unlikely to disrupt, and if the impulse from stand-off burst ablation is delta $v > 10\ v_{esc}$, the object is very likely to strongly disrupt. However, those statements do not predict what might happen in between that range, nor do they necessarily apply to contact bursts. The hypothetical threat object size range and orbits presented in the PDC 2025 scenario make it difficult to adhere to these delta V heuristics for stand-off bursts. This assumption drives mission design to high-risk scenarios involving many devices or impactors and many impulses in a way that we believe is unnecessary because this scenario allows rendezvous, which make proximal operations viable. Surface bursts

may be placed carefully in this scenario. They have the advantage of coupling much more energy to the target in a highly localized manner. This work tests the possibility of using far fewer devices to strongly disrupt a hypothetical threat object of this size.

The energy released from a nuclear device is essentially mediated by three different pathways, only two of which are relevant to the PHO problem. Kinetic energy of the blast debris from vaporized device and any material very near the device is more important on Earth than in space where there is no air near the device to absorb energy and cause a blast-wave. In space, x-rays carry most of the energy away from the point of detonation. High-energy neutrons from the nuclear reactions also mediate a small fraction of the energy.

The x-rays deposit their energy within the first several millimeters of the target surface. Depending on the device yield, the distance between the device and the target (the height of burst), and the heat capacity of the target regolith, a variety of things can happen. If the energy deposited is below the threshold required to vaporize the target material, then it simply feels a force from the radiation pressure and thermal expansion as the material heats up. As the energy deposited increases beyond that required to vaporize the target material, some of the vapor may continue to heat up to very high temperatures. Neutrons deposit energy in a target at much greater depths than do x-rays. This thicker deposition region has the potential to result in a larger amount of material being mobilized from the target surface, either as vapor or solid debris. However, the fraction of the total energy yield from a nuclear device that is mediated by neutrons is significantly smaller than that mediated by x-rays. Approximately 97% of the energy emitted from a nuclear device is in the form of kinetic energy (debris) and thermal radiation (x-rays). We model this portion of the device energy using the Pagosa hydrocode.

Glasstone and Dolan [4] developed scaling methods to make explosion crater dimension predictions based on nuclear test data. Their scaling relations suggest that disruption of 2024 PDC by a near-surface burst is possible. By their method, transient crater dimensions measured after 1 kt nuclear detonations at various depths and heights of burst are compiled and scaled to other yields and heights or depths of burst. They find that the transient crater depth and diameter scale approximately as $Y^{1/3}$. For the specific question of a Y = 1 MT surface burst over dry soil or dry soft rock, the scaled depth of burst (DOB) is

$$\text{DOB}/(\text{Y}\text{\^{}}(1/3)) = 0/(1000^{1/3}) = 0. \quad (1)$$

The scaled diameter of the transient crater is predicted to be

$$\text{D}(1\text{ kt, DOB}) \times \text{Y}^{1/3} = 37*(1000^{1/3}) = 370\text{ m} \quad (2)$$

scaling from the 1 kt burst data plotted in Fig. 1. The scaled depth of the transient crater is predicted to be

$$\text{d}(1\text{ kt, DOB}) \times \text{Y}^{1/3} = 8.5*(1000^{1/3}) = 85\text{ m} \quad (3)$$

from the 1 kt burst data plotted in Fig. 2, noting that both figures are plotted in imperial units. The crater predicted by this method is comparable to the size of the largest predicted point case instantiation of 2024 PDC predicted by Dotson at ATAP [5]. While the predicted crater depth is less than the length of the predicted short axes of 2024 PDC, we note that this model does not scale for surface gravity in the way that

Holsapple's scaling relations do [6], so we would expect the crater to be even larger in microgravity. Neglecting that advantage, it would still require significant strength for the target object to resist disruption of the remaining material in such a cratering event. Below, we show that the threat object would have to be stronger than steel to resist disruption in this scenario.

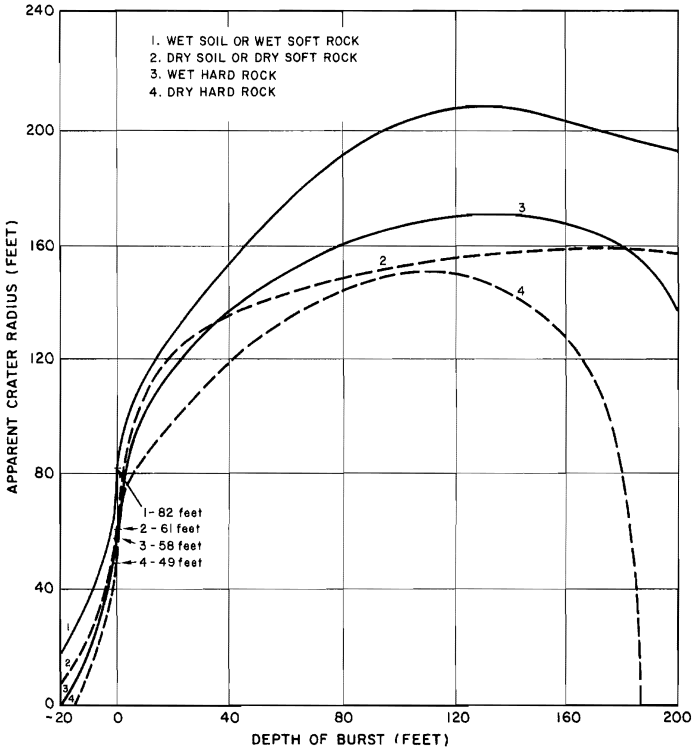

Figure 1: Explosion crater radii vs depth of burst measured for 1 kt explosions, Fig. 6.72a from [4] p. 255.

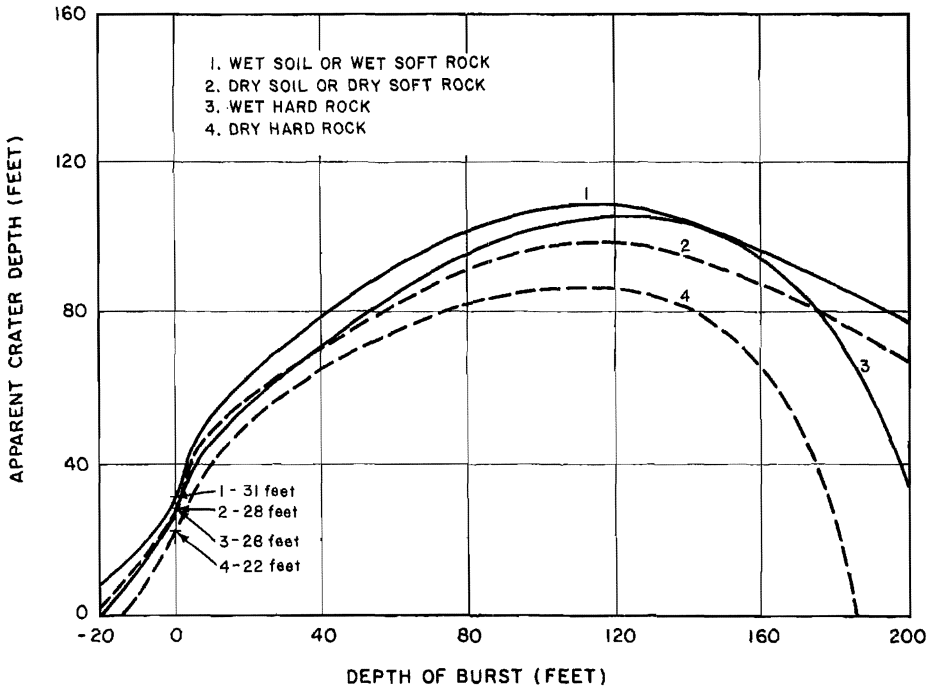

Figure 2: Explosion crater depth vs depth of burst measured for 1 kt explosions, Fig. 6.72b from [4] p. 256.

The amount of material displaced in a strong disruption should be predicted to be at least that of a similarly sized *transient* crater. The transient crater is that which exists at the end of the excavation stage on a planetary body. It is deeper and narrower than the final crater. Over geologic time on Earth, the transient crater slumps, becoming wider and shallower. The modification process does not apply to our disruption scenario, so we use the transient crater, not the final crater as our metric. We hypothesize that if the device is big enough to move at least that much material on Earth, it should do so in space. A 1 MT contact burst on the threat object is not expected to make a smaller crater for several reasons. First, the target has lower surface gravity and no air to resist the excavation. Second, the threat object is expected to be weaker than the rock under load used in the experiments that Glasstone and Dolan's model is calibrated to. Third, the strong shock and release waves propagate through the entire target body, while the explosions on Earth can be thought to have an effectively infinite amount of material below the cratering surface to catch the material below the excavating crater.

Koa crater on Eniwetok Atoll is a potential near neighbor to such an explosion. It is described in [7]. The Koa experiment had a yield of 1.3 MT, a final crater diameter of 1.1 km, a transient crater diameter of 400-500 m, and an excavation depth of 41 m. Extensive studies of the crater were done by the USGS PEACE Program in the 1980's [8].

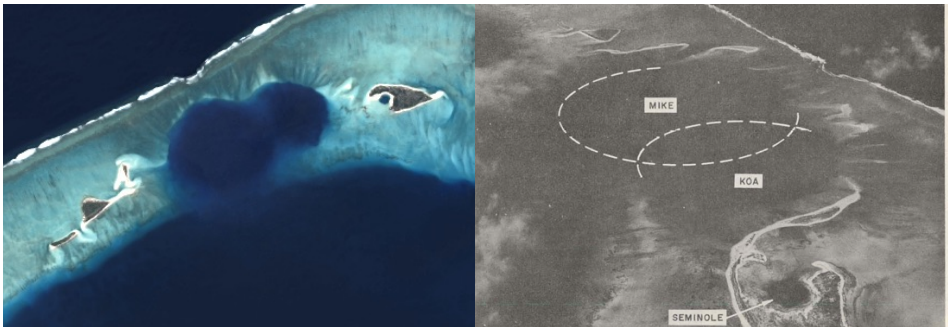

Figure 3: Left: Landsat image of Eniwetok Atoll, showing the Mike and Koa craters. (NASA/USGS), Right: Frontispiece of [7], showing the Koa, Mike, and Seminole crater locations.

Methods

We don't know the internal properties of 2024 PDC, or most asteroids, well enough to constrain high-fidelity numerical models of their internal structures, so we present a 'steel man' case to test our hypothesis. A 'steel man' is a rhetorical technique used to address the strongest form of an argument. In this case, we take literal steel as the strongest form of the hypothetical threat object. Specifically, we believe 2024 PDC to be structurally weaker than solid SAE 304 stainless steel [9], as shown in Table 1. We can then model 2024 PDC as solid steel, which has well-known constitutive properties that are frequently used and well-validated in hydrocode calculations [10]. If a steel target disrupts in our models, we believe the scenario would likely also disrupt an S-type 2024 PDC hypothetical threat object.

Material	**Yield**	**Tensile**	**Shear**
S-type	0.2-5 MPa	< 10 MPa	< 10 MPa
SAE 304	294 MPa	200 MPa	370 MPa

Table 1: A comparison of rough values of strength for steel and S-type asteroids.

For our 'steel man' hypothetical threat object, we use the 2024 PDC 95th percentile ellipsoid (121m x 124 m x 236 m) point case volume but make the target out of homogeneous solid steel using the Sesame EOS 4272 [11], shown in Fig. 4. Steel has a density of 7.91 g/cc, which is 3x the density (and mass, for identical volumes) of the 95th percentile point case. We use a Preston-Tonks-Wallace strength model [12] and Johnson-Cook damage model [13] with constitutive properties shown in Table 1.

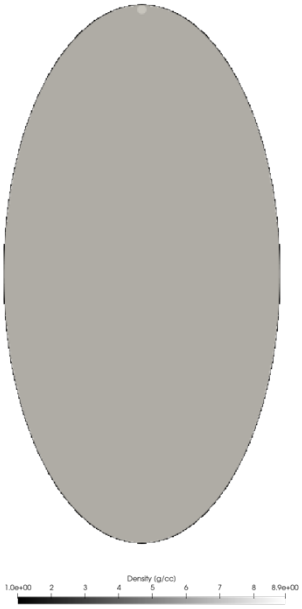

Figure 4: A 2D cross-section of the initial Pagosa mesh at t = 0, plotted by density. The target is modeled as SAE 304 steel of the same volume as the 95th percentile point case predicted for 2024 PDC. The small circle at the top is the energy pill.

The energy pill is a 2-m-diameter sphere of Mie-Gruenisen copper placed at the surface so that it is partially buried along the long axis of the target. The material is an arbitrarily chosen metal with a well-validated EOS. The burst energy is sourced into the internal energy of the region at t=0, and the pill is allowed to respond thermodynamically according to the EOS. We intentionally placed it on the long axis of the target as the most pessimistic placement for shock propagation, in keeping with our steel man hypothesis testing philosophy. We conducted a parameter study over energy pill yield from 1 ton TNT < Y < 500 kt TNT to test the yield range over which the target disrupts or not, and to assure ourselves that a sensible lower bound exists at which the target is not predicted to disrupt.

For these simulations, we use the LANL ASC code Pagosa. Pagosa is a 1-3D Eulerian finite difference hydrodynamics code. It has a fixed (non-AMR) mesh and a variety of strength and damage models. It is used to study high-velocity impacts and high explosives phenomena [14]. Verification and validation of Pagosa for crater modeling was done by [15] Pagosa was also tested in the Stickle et al. [16] code benchmarking study prior to DART. Pagosa simulations use pure hydrodynamics without x-ray transport. The models conducted for this work were done in 2D axi-symmetry with 50 cm fixed mesh cells.

To consider a target mitigated for our purposes here, we require that the initial target parameters should over-predict the difficulty of disruption, no remaining fragment should be larger than 30 m, which is the lower bound predicted impactor diameter of Tunguska, and any remaining fragments should be left with sufficient velocity to miss Earth. This last criterion is not well-posed. Further study is needed on the amount and fragment size distribution of disrupted mass that could tolerably impact Earth in each scenario. Each scenario will also have a unique threshold miss-velocity for fragments too large to be significantly affected by the solar wind, based on that scenario's orbital dynamics.

Results

The parameter study over energy pill yield ranges from 500 kt to 1 ton TNT of internal energy. The results of our parameter study are listed in Table 2. We find that the hypothetical threat object is thoroughly disrupted by the energy pill initialized with 500 kt of internal energy and is not disrupted by energy pills initialized with internal energies less than 10 kt. For our disruption prediction above, we double the yield requirement because we expect pill models to over-predict the amount of energy available to do PdV work on the solid (non-ablated) portion of the target. Although we may be able to decrease the yield required to disrupt through higher-fidelity models if mission requirements needed us to relax that threshold, we do not expect a yield higher than that physically required to strongly disrupt a threat object to disrupt that object any less thoroughly.

(Author's note: The 10 kt, 100kt, and 200kt cases are still running as of April 22, 2025. The results of these simulations will be added as they finish, which is anticipated to be well in advance of the final paper submission date. Unavailable values are marked TBD for "to be determined" for now.)

Yield (kt)	**Disrupted?**	**Q^*_D Achieved?**	**dV >100 cm/s?**	**Energy Imparted**
500	Yes, t < 0.4 s	Yes, t < 0.2 s	Yes, t < 0.1 s	170 kt deposited, ~50 kt does work on solids
200	TBD	TBD	TBD	60 kt deposited, ~ 30 kt does work on solids
100	TBD	TBD	TBD	30 kt
10	No	No	No	3.7 kt
1	No	No	No	0.55 kt
0.001	No	No	No	~10 lbs TNT

Table 2: Results of the parameter study of contact bursts of various yields against a target of the same volume as the 95th percentile point case of 2024 PDC but made of SAE 304 steel with strength and damage calculations included in the models.

For the 500kt case, we plot all cells whose total damage remains below d =1, or full damage, throughout the calculation in Fig. 5. We see that there are no contiguous regions that are 30 m (60 cells) across or larger within the target. The target material is thoroughly damaged and has a radial velocity greater than 1 m/s at late time, so we expect the damaged material to thoroughly disperse.

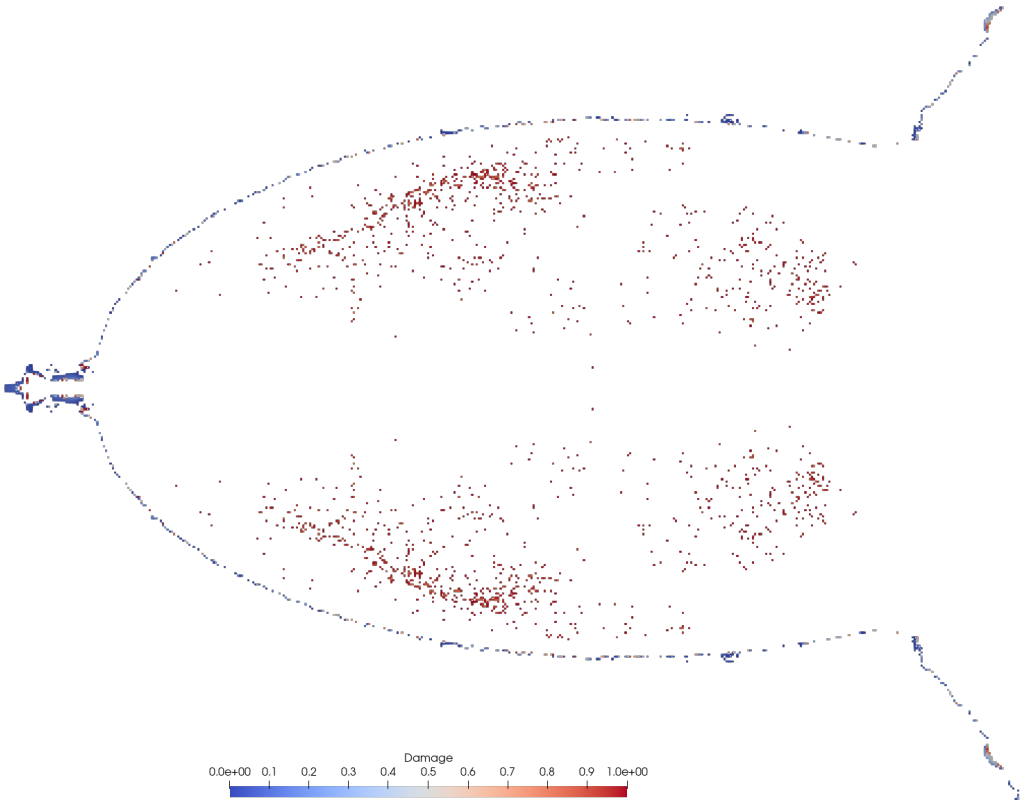

Figure 5. Cumulative damage plot at late time from the 500 kt simulation, showing half of a 2D cross-section, where the energy pill was originally to the right, thresholded to only show cells that were never fully damaged.

The cases with pill energies below 10 kt do not disrupt, and do not predict partial disruption, as detailed in Tab. 3. In Fig. 6, the target is damaged, but only small regions near the burst and at the distal end of the target show complete material failure at late times when the shock pressure has fallen between P_{fail} = -5.9e4 MPa and Y_0 = 200 MPa, the range in which we don't expect further damage to occur. The target in these cases would be expected to remain in one piece, with cracking near the burst end and antipode. The lower energy cases do not tell us about the response of an S-type target, but they do give us confidence that the strength model in our simulations is controlling the disruption of the targets in the ways we expect it to.

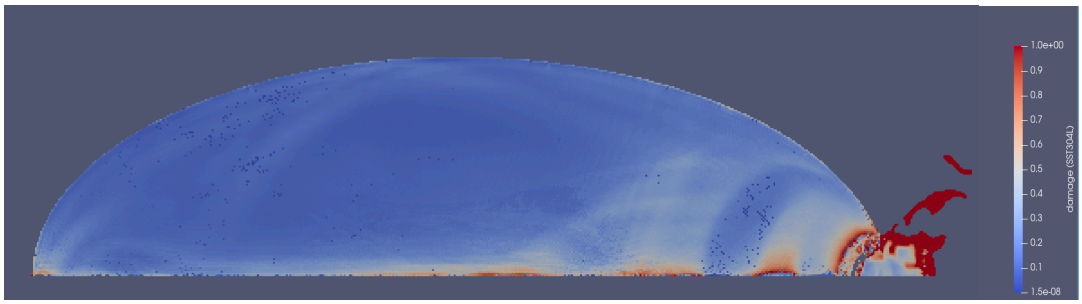

Figure 6: Damage plot at late time, after the shocks have attenuated below the level at which the material would be further damaged, from the 1 kt simulation, shows a lightly damaged contiguous body.

Yield (kt)	First shock crossing	Time shock attenuated to $-P_{fail} < P < Y_0$	Damage at time of attenuation
10	t = 0.0383 s	t > 0.07 s	TBD
1	t = 0.0387 s	t = 0.0676	minimal
0.001	t = 0.0412 s	t = 0.0412	minimal

Table 3: Time thresholds for shock crossing and attenuation and damage assessments for the steel models with yields low enough that they do not predict disruption of the target.

Conclusions

A single 500 kt – 1 Mt contact burst appears sufficient to strongly disrupt a steel object of the same volume as the 95th percentile case of 2024 PDC based on the results of the scaling relations and numerical models presented here. We believe that this prediction also indicates that a 1 Mt contact burst should be sufficient to disrupt any instantiation of the S-type 2024 PDC hypothetical threat object. The lower bound estimate of the energy required to mitigate is presented for completeness. It does not drive mission design for this scenario. A higher yield is not expected to reduce the efficacy of the disruption. A lower yield could be carefully considered if mission requirements made that desirable.

Strong disruption of the threat object may be desirable for a variety of reasons when the option is available. Disruption is relatively insensitive to timing and direction relative to the threat object's orbit, if sufficient time is allowed for the debris to disperse. Further studies on the requirements for mitigation by strong disruption are needed, especially the amount and fragment size distribution of remaining debris that would be acceptable if it remained on an Earth-impacting trajectory. Additional further studies on the specific case of a contact binary are also needed. It is plausible that a multi-device mission with 2-3 devices to be placed on the surface, or a fleet of 2-3 single-device spacecraft detonated simultaneously at carefully chosen locations could strongly disrupt such an object without allowing large portions to remain undisrupted. Further study will doubtlessly reveal even better solutions to this engineering problem.

For the PDC 2025 emergency response exercise, using mission schedules developed by [5], we believe that mitigation by strong disruption is possible and could be used as a main mitigation option from 2032-2039, which would allow 5+ years of development and spacecraft integration time prior to launch. *If it were developed in parallel* to a different main option, it could be used as a reserve option in case of mission failure for ion beam deflection (IBD) from 2034-2039, or kinetic impactors from 2037-2039, while still allowing roughly time for construction and post-disruption debris dispersal. If the contact burst option was not developed in parallel to the main option, then a contact burst mission could plausibly be developed for use in 2039 after the failure of an IBD mission in 2034 or 2035. Mission development would need to be dramatically accelerated for main option failures after that time if the contact burst reserve option was not developed in parallel to the main mission.

Acknowledgements
This work, LA-UR-25-24088, was supported by the U.S. Department of Energy through the Los Alamos National Laboratory. Los Alamos National Laboratory is operated by Triad National Security, LLC, for the National Nuclear Security Administration of U.S. Department of Energy (Contract No. 89233218CNA000001).

References

(1) E. Teller, L. Wood, M. Ishikawa, R. Hyde, Threat object-dispersing approaches to active planetary defense, in: Cosmic bombardment V, USDOE, 1994.
(2) T. J. Ahrens, A. W. Harris, Deflection and fragmentation of NEAs, in: T. Gehrels, M. S. Matthews, A. M. Schumann (Eds.), Hazards Due to Comets and Asteroids.
(3) J. C. Solem, “Interception and Disruption”, Planetary defense workshop, Livermore, CA (United States), 22-26 May 1995.
(4) S. Glasstone, P. J. Dolan, The Effects of Nuclear Weapons, U.S. Government Printing Office, 1977, pp. 253-257
(5) B. Barbee et al., “NASA Analysis of Space Mission Options for the 2025 Planetary Defense Conference Hypothetical Asteroid Impact Threat Scenario”, 2025 Planetary Defense Conference, IAA-PDC-25-01-87, May 2025.
(6) K. A. Holsapple and R. M. Schmidt, “On the scaling of crater dimensions: 2. Impact processes”, JGR Solid Earth 87:B3, March 1982.
(7) L. J. Circeo Jr., and M. D. Nordyke, Nuclear Cratering Experience at the Pacific Proving Grounds”, UCRL-12172, 1964.
(8) T. W. Henry and B. R. Wardlaw, “Pacific Enewetak Atoll Crater Exploration (PEACE) Program Enewetak Atoll, Republic of the Marshall Islands, Part3: Stratigraphicanalysisandothergeologicandgeophysical studies in vicinity of OAK and KOA craters”, USGS Open File Report 86-555, 1987.
(9) AISI 304 (S30400) Stainless Steel material data sheet, https://www.makeitfrom.com/material-properties/AISI-304-S30400-Stainless-Steel accessed April 2025.
(10) T. Heberling et al., “Hydrocode simulations of a hypervelocity impact experiment over a range of velocities”, Int. J. IE vol. 122, p. 1-9, 2018.
(11) J. C. Boettger, “SESAME Material 4272: Stainless Steel”, 2001.
(12) D. Preston, D. Tonks, D. Wallace. “Model of Plastic Deformation for Extreme Loading Conditions.” Journal of Applied Physics, 93, 211 , 1999.
(13) G. Johnson, W. Cook. “A Constitutive Model and Data for Metals Subjected to Large Strains, High Strain Rates, and High Temperatures.” In Proceedings of Seventh International Symposium on Ballistics, pp. 541 – 548. The Hague, The Netherlands, 1983.
(14) Weseloh, Wayne N., Sean P. Clancy, and James W. Painter. *PAGOSA physics manual*. No. LA-14425-M. Los Alamos National Laboratory (LANL), Los Alamos, NM (United States), 2010.
(15) Heberling, Tamra, et al. "Calculating the momentum enhancement factor for asteroid deflection studies." *Procedia Engineering* 204 (2017): 124-129.

(16) Stickle, Angela M., et al. "Benchmarking impact hydrocodes in the strength regime: Implications for modeling deflection by a kinetic impactor." *Icarus* 338 (2020): 113446.